

# ELECTROCLINIC LIQUID CRYSTAL MATERIALS FOR ELECTROOPTIC IMAGING

*J. Naciri, G. Crawford, R. Shashidhar, and B.R. Ratna*

*Center for Bio/Molecular Science and Engineering, Code 6950  
Naval Research Laboratory, Washington DC 20375 USA*

## Abstract

The correlation between molecular structure and electrooptic performance is studied for two series of ferroelectric liquid crystalline materials. The first series (Series 1) consist of siloxy units attached to the hydrocarbon chain at the non-chiral end of the molecule; while the second series (Series 2) contain only hydrocarbon chains at the end of the molecule. Series 1 exhibit chiral smectic A (SmA) and smectic C (SmC<sup>\*</sup>). It is observed that slight modifications in either the siloxy or the hydrocarbon chain length has strong effect on the electro-optic properties. Increasing the number of siloxy unit in the chain (Series 1) increases the temperature range of SmA, and reduces the SmA-SmC<sup>\*</sup> transition temperature. All materials have melting temperatures below room temperature, and exhibit high values of induced tilt angles. In Series 2, the materials show a broad SmA temperature range, and melting temperatures much higher than in Series 1. However, the SmA phase is found to supercool to subambient temperatures. If the hydrocarbon chain is shortened, tilt angle, electroclinic coefficient and switching time are significantly suppressed. Comparison of the electrooptic performance in SmA between the two series show that Series 1 show a much higher tilt angles than Series 2, while the later exhibit much faster response times.

## Introduction

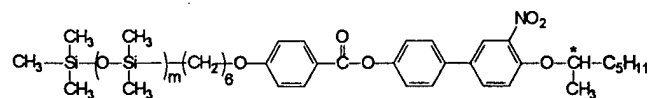
Chiral smectic A electroclinic liquid crystalline materials are prime candidates for electrooptic applications because of their gray scale capability and fast dynamic response<sup>1</sup>. The limiting features of electroclinic materials for use in applications thus far have been low induced tilt angles which result in low contrast ratios and narrow temperature range of the SmA phase at temperature above ambient. Development of materials with large electroclinic tilt angles needed for applications requires a fundamental understanding of the relationship between the molecular

structure and the magnitude of the induced tilt angle<sup>2-4</sup>. Bahr, Heppke, and Klemke<sup>2</sup> studied a homologous of materials to probe the relationship between molecular structure and the electrooptic performance. They observed that a longer alkyl chain on the non-chiral end resulted in a larger electroclinic tilt angle. Walba and coworkers<sup>5</sup> have pioneered studies of mixtures of these new electroclinic materials with compounds which exhibit a SmC<sup>\*</sup> phase to enhance their electrooptic response and tilt angle.

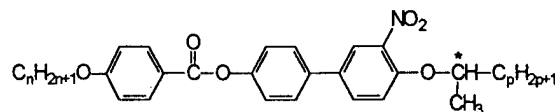
In this contribution we report the electrooptic performance of two series of ferroelectric liquid crystalline materials. The results show that slight modifications of the chain at the non-chiral of the molecule result in dramatic differences in their electrooptic performance. In particular, the organosiloxane liquid crystalline series exhibit properties that make them very attractive for applications: low melting temperature and high-induced tilt angle values.

## Materials and Synthesis

The general structures of the materials are shown in Fig. 1 and the synthesis steps leading to their preparation are illustrated in Scheme 1-3.

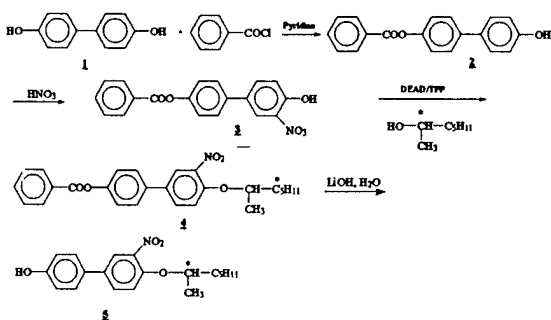


Series 1      mSiKN65      m=0, 1, 2

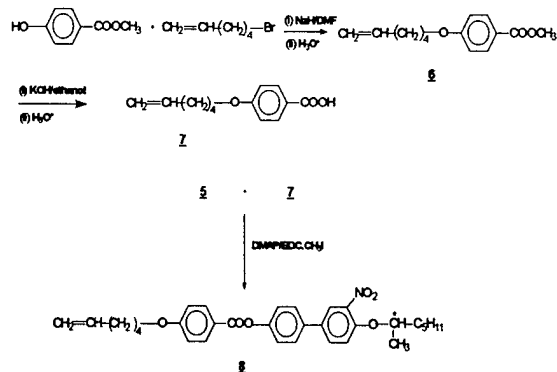


Series 2      KNnp      n=8, 10, 12      p=3, 4, 5, 6

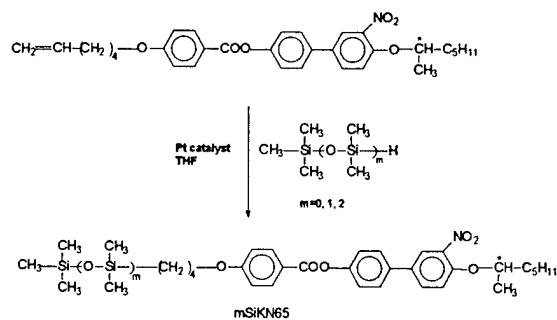
Figure 1: Molecular structure of electroclinic materials



Scheme 1



Scheme 2



Scheme 3

The phenol ring of compound **2** was then selectively nitrated using nitric acid in acetic acid. Nitrophenol **3** was then coupled with (R)-2-heptanol using the stereospecific Mitsunobu coupling procedure to give compound **4**. Deprotection of the phenol by hydrolysis of the benzoate ester with hydroxide ion then gave compound **5**. The carboxylic acid derivative **7** was prepared by reacting hydroxybiphenyl carboxylic methyl ester with 6-bromo-1-hexene in the presence of NaH. The mono-benzoyl ester **2** was prepared by reacting biphenol **1** with benzoyl chloride in pyridine, followed by hydrolysis. The vinylic derivative material **8** was obtained by esterification of the carboxylic

acid derivative **7** with **5** in the presence of 1-(3-dimethylaminopropyl)-3-ethylcarbodiimide methiodine (EDC.CH<sub>3</sub>I) and dimethylaminopyridine (DMAP). The corresponding siloxy liquid crystalline materials were obtained through the classical hydrosilylation reaction between the vinyl mesogenic groups and hydrosiloxane derivatives in the presence of a Pt-catalyst (Scheme 3).

## Experimental

For electrooptic studies and tilt angle measurements, the materials were loaded into prefabricated 4  $\mu\text{m}$  commercially available samples cell (E.H.C., Japan) without further processing. The indium oxide (ITO) coated glass plates had an overlying rubbed polyimide alignment layer to facilitate uniform planar alignment. The temperature of the sample was controlled in a Mettler hot stage.

The electric field induced molecular tilt angle,  $\theta$ , was measured by monitoring the concomitant change in relative intensity,  $\Delta I$ , and zero-field intensity,  $I_0$  when the homogeneously aligned sample was oriented between crossed polarizers with the first polarizer being oriented at an angle  $\gamma$  with respect to the director in the absence of the field as depicted in Fig. 2. By orienting the sample at an angle  $\gamma = \pi/8$ , the tilt angle can be readily derived by the simplified expression  $\theta = \sin^{-1}(\Delta I/I_0)/4$ , where  $\Delta I = I_{\text{max}} - I_{\text{min}}$  corresponds to the difference between the maximum,  $I_{\text{max}}(V_0)$ , and minimum,  $I_{\text{min}}(-V_0)$ , intensity at a voltage  $V_0$  and  $-V_0$ .<sup>6</sup> The  $\gamma = \pi/8$  orientation of the sample was chosen because it is most sensitive to the angular position of the director, therefore enabling even small tilt angles to be determined precisely. The transmitted light intensity through the sample was monitored with a photodiode and digital oscilloscope. We have recently modified the analysis of the measured intensity to derive the molecular tilt angle even if the quasi-bookshelf stripe texture is present. This correction becomes important for materials with a large induced tilt angle (large electric field) and is negligible for small tilt angles. However, this requires additional information on the quasi-bookshelf geometry which is only accessible with x-ray diffraction techniques; therefore, we assume the bookshelf structure to derive our tilt angles. The tilt angle measurements were also checked by manually rotating the sample between crossed polarizers and identifying the extinction states corresponding to  $+V_0$  and  $-V_0$  to ensure the accuracy of our intensity measurements.

## Result and Discussion

The transition temperatures of the two series of materials are shown in Table 1. For series I, the SmA-Isotropic transition of all materials remains practically the same, and the melting points are very low. This lack of

crystallinity seems to be associated with the flexibility of the siloxane chains. It is also interesting to note that the presence of a single siloxy unit induces a smectic C<sup>\*</sup> phase in the material. However, increasing the number of siloxy units appears to restabilize the SmA phase by reducing the SmA-SmC<sup>\*</sup> transition temperature (Table 1). In series 2, the materials show a broad SmA temperature range, and

Compound	Phase sequence (°C)
<b>Series 1</b>	
m=0 SiKN65	SmC <sup>*</sup> 48.2 SmA 51 I
m=1 DSiKN65	SmC <sup>*</sup> 40.5 SmA 55 I
m=2 TSiKN65	SmC <sup>*</sup> 23 SmA 55.5 I
<b>Series 2</b>	
KN123	K <-5 SmA 81.4 I
KN124	K 15 SmA 79.3 I
KN125	K 29.8 SmA 80 I
KN105	K 45 SmA 76.4 I
KN106	K 39 SmA 74 I
KN86	K 58.9 SmA 68.7 I

Table 1: Phase transition temperatures for Series 1 and 2. The crystal and isotropic phases are denoted by K and I.

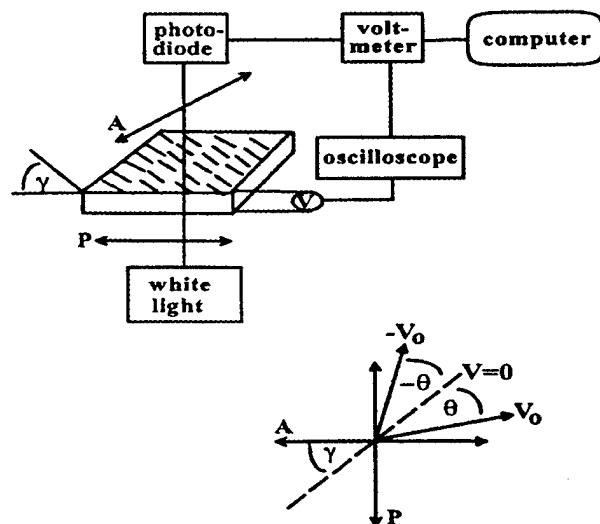


Figure 2: Experimental apparatus for electrooptic characterization

melting temperatures much higher than in series 1. However, the SmA phase is found to supercool to subambient temperatures.

We have measured the induced tilt angle in the chiral smectic A phase as a function of electric field at several temperatures for the TSiKN65 (m=2) and DSiKN65 (m=1) materials. We did not perform such measurements

on the SiKN65 material because of the somewhat narrow chiral smectic A temperature range. Figures 3 and 4 show data on the dependence of the electroclinic tilt angle on the applied electric field ( $E_{app}$ ) for TSiKN65 and DSiKN65 respectively. Both materials exhibit similar trends except for temperatures very close to the SmA-SmC<sup>\*</sup> transition. The tilt angle is a linear function of  $E_{app}$  for higher temperatures but departs from the linear behavior at lower temperatures. This departure from linearity is more pronounced for DSiKN65 (Figure 4) than for TSiKN65 (Figure 3). The tilt angles at the maximum voltage ( $6 \text{ V } \mu\text{m}^{-1}$ ) shown in Figure 3 and 4 are similar for the two materials  $\sim 14^\circ$  for TSiKN65 and  $\sim 15^\circ$  for DSiKN65. However, there is an important difference; while the tilt angle is saturated for DSiKN65 at about  $6 \text{ V } \mu\text{m}^{-1}$ , it still shows an increasing trend for TSiKN65 at  $E_{app} \sim 6 \text{ V } \mu\text{m}^{-1}$ . The switching time,  $\tau$ , was measured by recording the optical of the material as it traversed from  $-\theta$  to  $\theta$  (using a bipolar pulse from  $-V_0$  to  $V_0$ ), as the time that elapsed from 90% transmission state to the 10% transmission state. Data on the field dependence of the electroclinic switching times ( $\tau$ ) at different temperatures are shown in Figures 5 and 6. For TSiKN65 (Figure 5), the profile of  $\tau$  versus  $E$  is nearly flat. This field independent behavior of  $\tau$  is similar to that observed in other electroclinic materials<sup>7</sup> at temperatures far from SmA-SmC<sup>\*</sup> transition. The switching time for DSiKN65 (Figure 6) also shows a somewhat flat profile, but only away from the SmA-SmC<sup>\*</sup> transition. At these temperatures  $\tau$  for DSiKN65 is substantially less than that for TSiKN65. At  $43^\circ \text{ C}$ , which is about  $2^\circ$  from the transition,  $\tau$  exhibits a pronounced dependence on electric field with the response time decreasing with increasing field. This trend which indicates a departure from the soft-mode like dynamics of the smectic A, could be due to a pronounced tilt order developing close to the SmA-SmC<sup>\*</sup> transition. Such an increasing trend is also predicted by models for materials with large induced tilt angles<sup>8</sup>.

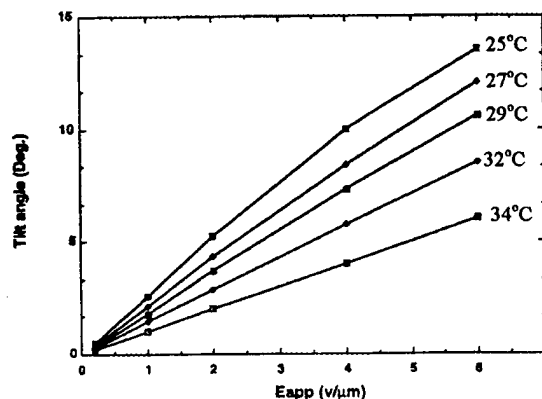


Figure 3: Induced tilt angle for TSiKN65 in SmA as function of electric field at several temperatures.

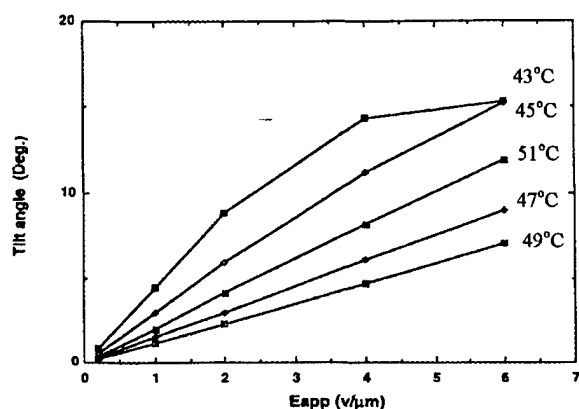


Figure 4: Induced tilt angle for DSiKN65 in SmA phase as function of electric field at several temperatures.

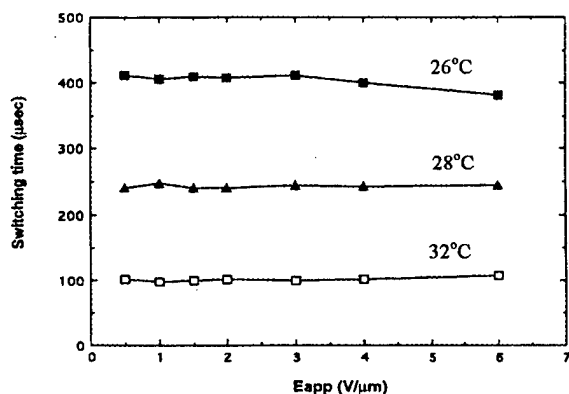


Figure 5: Switching time of TSiKN65 as a function of electric field at several temperatures.

The induced tilt angle as a function of electric field for series 2 is presented in Fig. 7. The first comparison to make is between KN125, KN124 and KN123. Decreasing the hydrocarbon chain on the chiral side results in a substantial decrease in the molecular tilt angle and changes the profile of the  $\theta$  versus  $E$  curves. The tilt angles for KN125 and KN124 materials start out very linear and increase less rapidly at  $E=2$  V/ $\mu\text{m}$  eventually reaching a value of  $\theta \sim 15^\circ$  at  $E=10$  V/ $\mu\text{m}$ ; however KN123 tilt angle maintains a very linear profile for fields up to  $E=10$  V/ $\mu\text{m}$  but only reaches a tilt angle of  $\theta \sim 5^\circ$ . The value of  $d\theta/dE=0.27$   $^\circ$ /(V/ $\mu\text{m}$ ), compared to  $d\theta/dE=4.7$   $^\circ$ / $\mu\text{m}$ ) for KN125 at low fields. A similar comparison can be made between KN106 and KN86. Decreasing the hydrocarbon

chain at the non-chiral side of the molecule results in a decrease in the tilt angle value.

The switching times,  $\tau$ , for all materials are fast and vary from 40  $\mu\text{sec}$  to 70  $\mu\text{sec}$ . The value of  $\tau$  for KN124, KN125 and KN106 materials are found to be strongly dependent on the electric field, whereas  $\tau$  for other compounds exhibit field independent switching behaviors.

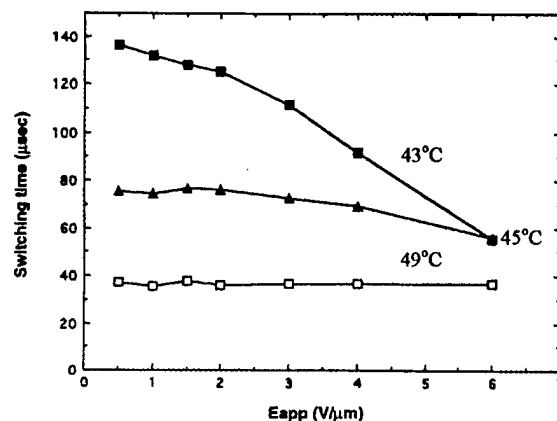


Figure 6: Switching time of DSiKN65 as a function of electric field at several temperatures.

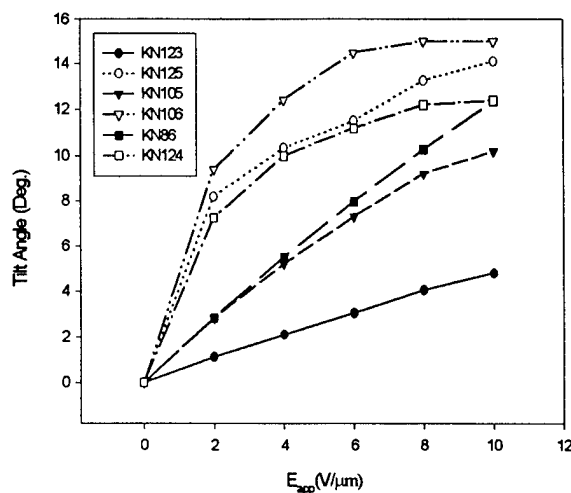


Figure 7: Molecular tilt angle as function of electric field at  $T=25^\circ\text{C}$

## Conclusions

We have studied the electroclinic effect of two series of liquid crystalline materials. In series 1, the electrooptic properties are very sensitive to the number of siloxy units attached to the hydrocarbon chain at the non-chiral end of the molecule. These materials exhibit unusually large electroclinic coefficient, even at temperatures well in the SmA phase. The presence of the siloxy groups decreases the crystallization temperature drastically and maintains low switching times even at ambient temperatures. In series 2, the electrooptic performance strongly depends on the length of the hydrocarbon chain. The molecular tilt angle and electroclinic coefficient were found to decrease with decreasing chain length. All materials presented here were stable at ambient temperatures, and therefore, have great potential for applications.

## References

1. N. A. Clark and S.T. Lagerwall: *Ferroelectric Liquid Crystals: Principles, Properties and Applications* (Gordon and Breach Science, Philadelphia), 1991.
2. C. H. Bahr, G. Heppke, and U. Klemke, *Ber. Bunsenges. Phys. Chem.*, **95**, 761 (1991).
3. B. R. Ratna, G. P. Crawford, S. Krishna, J. Naciri, P. Keller, and R. Shashidhar, *Ferroelectrics*, **148**, 425 (1993).
4. B. R. Ratna, G. P. Crawford, J. Naciri, and R. Shashidhar, *Proc. SPIE*, **2175**, 79 (1994).
5. D. M. Walba, D. J. Dyer, R. Shao, N. A. Clark, R. T. Vohra, W. N. Thumes, and M. D. Wand, *Ferroelectrics*, **148**, 435 (1993).
6. S. D. Lee, and J. S. Patel, *Appl. Phys. Lett.*, **54**, 1653 (1989).
7. G. Anderson, I. Dahl, W. Kuczynski, S. T. Lagerwall, K. Skarp, and B. Stebler, *Ferroelectrics*, **84**, 285 (1988).
8. I. Abdulhalim, and G. Moddel, *Liq. Cryst.*, **9**, 493 (1991).